Optics Letters

Chaotic optical communications over 100-km fiber transmission at 30-Gb/s bit rate

Junxiang Ke,[1] Lilin Yi,[1,*] Guangqiong Xia,[2] and Weisheng Hu[1]

[1]State Key Laboratory of Advanced Optical Communication Systems and Networks, Shanghai Institute for Advanced Communication and Data Science, Shanghai Jiao Tong University, Shanghai 200240, China
[2]School of Physics, Southwest University, Chongqing 400715, China
*Corresponding author: lilinyi@sjtu.edu.cn

Received 27 December 2017; revised 14 February 2018; accepted 19 February 2018; posted 20 February 2018 (Doc. ID 318491); published 12 March 2018

For the first time, to the best of our knowledge, we experimentally demonstrate a successful 30-Gb/s signal transmission of a duobinary message hidden in a chaotic optical carrier over 100-km fiber. Thanks to the duobinary modulation format with high spectral efficiency, the 30-Gb/s signal can be encrypted by a 10-GHz-wide chaotic carrier. A digital signal processing technique can be used to convert duobinary data into binary data on the receiver side. This proposal lowers the requirement for wideband chaos generation and synchronization in high-speed long-distance chaotic optical communications, and fiber dispersion compensation can also be simplified, which has potential to be used in high-speed long-distance secure optical communications.

OCIS codes: (140.1540) Chaos; (060.4785) Optical security and encryption; (060.2330) Fiber optics communications.

https://doi.org/10.1364/OL.43.001323

Since the first demonstration of chaos synchronization in 1990, the chaos system, used as a hardware encryption method in optical communications, has drawn much attention [1]. Many schemes based on the nonlinearity of lasers and modulators have been proposed in optical secure transmission [2–13]. From the viewpoint of practical applications, the modulator-based chaotic system has the benefit of simplified synchronization. The first field trial of chaotic optical communications based on a Mach–Zehnder modulator (MZM) scheme has been successfully demonstrated to support 2.4-Gb/s bit rate and 120-km transmission distance in Athens' metro-network [9]. Further, the first 10-Gb/s field experiment of chaotic optical communication based on a phase modulator and Mach–Zehnder interferometer (MZI) scheme over more than 100 km fiber has been successfully demonstrated [11].

However, chaotic optical communications encounter problems in high-speed and long-distance fiber transmission. First, the modulation formats used in the traditional chaotic optical communication systems are mainly on–off keying (OOK) and differential phase-shift keying (DPSK); therefore, a wideband chaos signal is needed for high-speed binary signal encryption. But the chaotic bandwidth of a laser-based chaotic system is limited by the relaxation oscillation, while the chaotic bandwidth of a modulator-based chaotic system is limited by the electrical devices. Therefore, many schemes have been proposed to generate wideband chaos [14–19]. But it is not easy to realize wideband chaos synchronization. Also, wideband chaos is very sensitive to fiber dispersion [20], which makes the synchronization quality become worse, and a part of the unsynchronized chaos signal is converted to noise, which makes the signal-to-noise ratio (SNR) become worse. Due to the above difficulties, there have been no demonstrations of chaotic optical communications beyond 10 Gb/s until now.

In this Letter, the difficulty of high-speed long-distance transmission described above can be solved; a 30-Gb/s secure signal transmission over 100-km single-mode fiber (SMF) based on 10-GHz optical and electrical devices is experimentally demonstrated. The message modulation format is duobinary, while the dispersion compensation fiber (DCF) and tunable dispersion compensation (TDC) module are used for dispersion compensation; an erbium-doped fiber amplifier (EDFA) is used for optical signal amplification. The performance of the system with different mask efficiencies has been studied in back-to-back (BtB) and 100-km transmission. Digital signal processing (DSP) is employed on the receiver side to convert duobinary into binary data for bit-error-rate (BER) measurement, and 30-Gb/s chaotic optical communications over 100-km transmission has been realized with BER less than 3.8×10^{-3}, which is the hard decision forward error correction (HD-FEC) threshold. We hope the proposed scheme can open a new window for high-speed and long-distance chaotic optical communications.

The experiment setup of the proposed scheme is illustrated in Fig. 1. A continuous-wave (CW) light with power of 14 dBm from a 1545-nm laser diode (LD2) with a narrow linewidth of 100 kHz is launched into a AVANEX MZM (MZM2) with a 3-dB bandwidth of 10 GHz and a half wave voltage of 3.8 V. The MZM2 provides nonlinear transfer function $\cos^2(x + \Psi)$, and the optical intensity of the injected light is modulated by the output of the broadband radio-frequency (RF) driver with a 3-dB bandwidth of 30 kHz–10 GHz, a gain of 45 dB, and maximum output peak-to-peak voltage of 10 V.

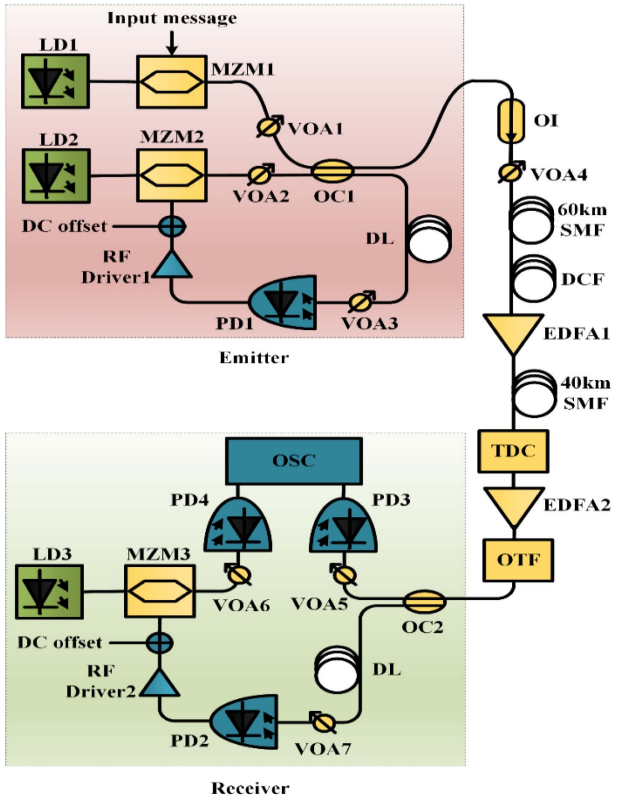

Fig. 1. Experiment setup. LD, laser diode; MZM, Mach–Zehnder modulator; VOA, variable optical attenuator; OC, optical coupler; DL, delay line; PD, photodiode; AMP, broadband radio frequency amplifier; OI, optical isolator; SMF, single-mode fiber; DCF, dispersion compensation fiber; EDFA, erbium-doped fiber amplifier; OTF, optical tunable filter; OSC, oscilloscope.

The output light of MZM2 is mixed with the output light from a 1545 nm LD1 with power of 14 dBm modulated by MZM1 driven by 30-Gb/s non-return-to-zero OOK (NRZ-OOK) pseudo random binary sequence (PRBS) signal; the 3-dB bandwidth of MZM1 is 10 GHz. Due to the bandwidth limitation of the modulator, the 30-Gb/s electrical binary data are converted to three-level duobinary data. The mixture ratio between chaotic carrier and message is controlled by a variable optical attenuator (VOA1 and VOA2). Through a 50:50 optical coupler (OC1), the light after mixture is split into two beams. One beam propagates for a few meters of optical fiber until it passes by the VOA3, which is used to control the feedback strength, then it is detected by a broadband amplifier photodiode (PD1) with a 3-dB bandwidth of 10 GHz and a responsivity of 125 mV/mW, and the input light power of PD1 is controlled at −5 dBm. The other output light of OC is used for transmission, and the optical isolator (OI) is used to prevent reflected light from the SMF, while the VOA4 is used to control the injection power of the fiber. The encrypted signal is transmitted for 60-km SMF with 11.7-dB insertion loss (IL), then a DCF with −936 ps/nm dispersion value and 3.7-dB IL is used to compensate the dispersion of SMF, and EDFA1 is used to compensate the transmission loss and control the injection power of the 40-km SMF with 7.8-dB IL. Then, a TDC with 5.1-dB IL and −764 ps/nm dispersion value is used for the accurate dispersion compensation, and the output light amplified by EDFA2 is filtered by a SANTEC optical tunable filter (OTF) with 3-dB bandwidth of 0.4 nm, which is used to suppress the amplified spontaneous emission (ASE) noise.

On the receiver side, the input light is split into two beams. One branch, consisting of VOA7, PD2, RF Driver2, LD3, and MZM3, is used for chaos republication, then the optical signal attenuated by VOA6 is detected by PD4 with 3-dB bandwidth of 10 GHz, and the physical parameters of PD2, RF Driver2, and MZM3 are the same as PD1, RF Driver1, and MZM2; the biases of MZM2 and MZM3 are set at $\pi/4$, while the wavelength of LD3 is also set at 1545 nm, and the output power of LD3 is set at 10 dBm. The other branch attenuated by VOA5 is directly detected by the PD3, which has the same physical parameter as PD4, and the output waveforms of PD3 and PD4 are collected by two 30-GHz bandwidth channels of an 80-GS/s LECROY SDA 845Zi-A oscilloscope (OSC). Then, the chaos synchronization is achieved in digital domain by calculating the correlation coefficient of two time series collected by the two channels of the OSC. After chaos synchronization, the decrypted 30-Gb/s duobinary data are converted to binary data for BER measurement. An Agilent N9010A electrical spectrum analyzer (ESA) with the bandwidth of 10 Hz–44 GHz is used to measure the RF spectrum of the signal.

The process of encryption can be represented by a mathematical model; the output signal I(t) of the emitter can be expressed as

$$I(t) = P_0 \cos^2\left(\frac{\pi G_e S_e \eta_e I(t-T) * h(t)}{2V_\pi} + \Psi_e\right) + \alpha P_0 m(t), \quad (1)$$

where [*] denotes the convolution operation, $h(t)$ is the impulse response of electronic feedback in the emitter, P_0 is the maximum optical power of chaos signal, T is the delay time of the feedback loop, η_e represents the IL of the feedback loop, S_e is the sensitivity of the photodetector, G_e is the gain of the RF driver, V_π is the half-wave voltage of MZM2, Ψ_e is the bias of MZM2, the duobinary signal $m(t)$ can be 0, 0.5, or 1, and αP_0 is the adjustable maximum optical power of the duobinary signal; therefore, the parameter α represents the masking efficiency of the message. In the experiment, VOA1 and VOA2 are used to tune the masking efficiency α.

First of all, the performance of chaos synchronization in the BtB situation has been studied, and the injection power of PD1 is controlled at −5 dBm by VOA3. In the meantime, the injection power of PD2 is finely tuned by VOA7 to get the same feedback strength as the emitter. Since the physical parameters of the device in the receiver are almost identical to the physical parameters in the emitter, the chaos republication can be realized in the receiver, then the time delay of two time series can be obtained by calculating the maximum correlation coefficient defined as Eq. (2); therefore, chaos synchronization between the emitter and receiver can be achieved. VOA5 and VOA6 are finely tuned to control the input power of PD3 and PD4 for optimal synchronization. As shown in Figs. 2(a) and 2(b), the chaotic time series of the emitter is very similar to the chaotic time series of the receiver. Then, the synchronization plot of the emitter output and receiver output is shown in Fig. 2(c), where chaos synchronization can be obviously observed. Further, the chaos synchronization is evaluated quantitatively, and the correlation coefficient, which is defined as Eq. (2), has been calculated:

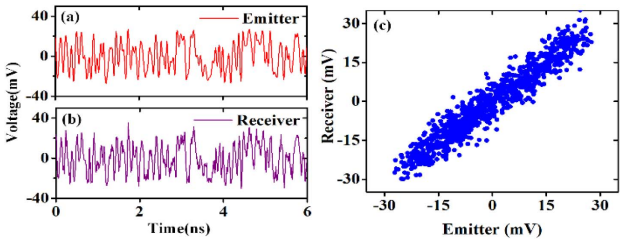

Fig. 2. (a) Time series of emitter; (b) time series of receiver; and (c) synchronization plot of emitter output and receiver output.

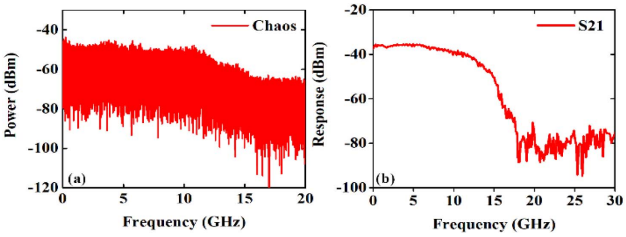

Fig. 3. (a) Spectrum of chaos signal and (b) S21 curve of system.

$$C = \frac{\langle [x(t) - \langle x(t)\rangle][y(t) - \langle y(t)\rangle]\rangle}{\sqrt{\langle [x(t) - \langle x(t)\rangle]^2\rangle \langle [y(t) - \langle y(t)\rangle]^2\rangle}}, \quad (2)$$

where $x(t)$ is the time trace of the emitter, $y(t)$ is the time trace of the receiver, and $\langle\cdot\rangle$ denotes average. The calculated correlation coefficient C is 96.44%. Also, The RF spectrum of the chaos signal is measured by ESA, as shown in Fig. 3(a), where the 3-dB bandwidth is about 10 GHz.

In order to generate the 30-Gb/s duobinary signal from the 30-Gb/s NRZ-OOK signal by the electrical filtering effect of the system, the system end-to-end bandwidth has been measured. First, in the BtB case, the electrical feedback loop in the emitter was disconnected, and a KEYSIGHT PNA Network Analyzer N5224A with 10 MHz–43.5 GHz was connected to the electrical port of MZM1 and the output of PD3. The S21 curve is shown in Fig. 3(b), and the 3-dB bandwidth of the system is about 9 GHz.

Then, we evaluate the system performance of the 30-Gb/s chaotic optical communications in the BtB situation. At the transmitter side, a 30-Gb/s NRZ PRBS15 signal from a KEYSIGHT N4960A pulse pattern generator (PPG) is directly measured by OSC and ESA. The eye diagram is shown in Fig. 4(a1), and the RF spectrum of the 30-Gb/s NRZ signal is shown in Fig. 4(a2). The eye diagram of duobinary data generated by the system bandwidth limitation is shown in Fig. 4(b1). The RF spectrum of the 30-Gb/s duobinary signal is also shown in Fig. 4(b2), which is consistent with the system bandwidth detected by electrical vector network analyzer (EVNA), while the spectrum of the duobinary signal can be masked by the spectrum of the chaotic carrier shown in Fig. 3(a). The duobinary signal encrypted by the chaotic carrier is shown in Fig. 4(c1), where the eye diagram cannot be recognized, since it is hidden by the chaotic noise, and the mask efficiency α is 1.45, while the RF spectrum of the encrypted signal is also shown in Fig. 4(c2). Compared with the duobinary signal, the spectrum of the encrypted signal becomes a

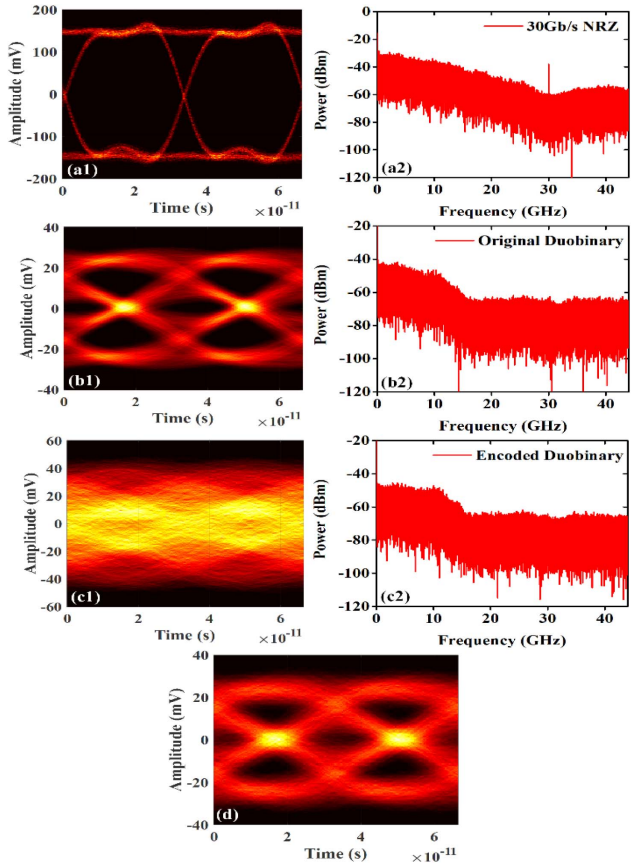

Fig. 4. (a1) Eye diagram of 30-Gb/s NRZ signal, (a2) RF spectrum of 30-Gb/s NRZ signal, (b1) eye diagram of 30-Gb/s duobinary signal, (b2) RF spectrum of 30-Gb/s duobinary signal, (c1) eye diagram of encrypted 30-Gb/s duobinary signal, (c2) RF spectrum of encrypted 30-Gb/s duobinary signal, and (d) eye diagram of decrypted 30-Gb/s duobinary signal.

little flatter, and the duobinary data are completely covered by the chaotic noise. Last, according to the waveforms measured by OSC from PD3 and PD4 at the same time, the duobinary message is recovered by synchronizing and subtracting the time series from OSC, and the recovered eye diagram is shown in Fig. 4(d), where the clear duobinary eye diagram can be achieved again.

Further, the chaos synchronization performance after transmission has also been studied. First, the performance of chaos synchronization after 60-km transmission is evaluated. TDC is used for dispersion compensation, EDFA is used to compensate the optical power loss, and the optical filter is used to remove the ASE noise. The dispersion compensation value is set at −1020 ps/nm at first, then the dispersion compensation value is slightly tuned to make sure of the best performance of chaos synchronization. In order to find the best injection power of the fiber, the relationship of correlation coefficient and injection power of the fiber is shown in the Fig. 5. When the injection power is too large, the nonlinear effect will become strong. But when the injection power is too low, the EDFA will introduce much ASE noise. Therefore, the injection power of the fiber is set at −4 dBm in the following experiment.

Last, the BER performance of 30 Gb/s duobinary chaotic optical communications for BtB and 100-km SMF is studied.

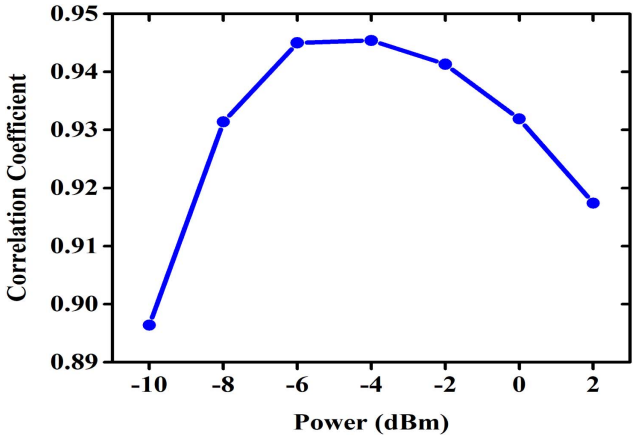

Fig. 5. Relationship curve between correlation coefficient and the injection power of fiber.

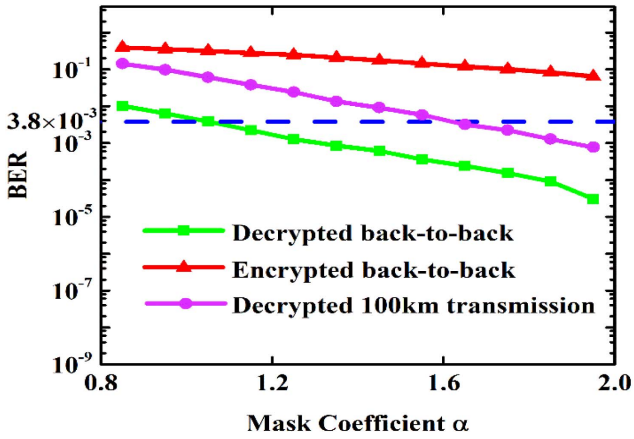

Fig. 6. BER performance of decrypted signal (green square) and encrypted signal (red triangle) in BtB situation, decrypted signal (purple circle) after 100-km transmission with different mask coefficient α. The blue dashed line is the threshold of HD-FEC.

The BER for the decrypted signal and encrypted signal in the BtB situation, and decrypted signal after 100-km transmission, with different mask efficiencies α, is calculated, which is shown in Fig. 6. The green line is the BER performance of the decrypted signal in the BtB case, where the BER decreases as the mask efficiency α increases, and the BER is below 3.8×10^{-3}, which is the HD-FEC threshold when the α is larger than 1.05. The BER performance of the encrypted signal is shown as the red line, which has the same tendency as the decrypted signal in the BtB situation, but the BER is always larger than 3.8×10^{-3} when the α is less than 1.95; therefore, the message cannot be recovered by direct detection. However, the system will become unsecure when α is very large according to the tendency. The BER performance of the decrypted signal after 100-km transmission is the purple line. Therefore, compared with the BtB case, there is BER degradation after 100-km transmission, but the BER is below the 3.8×10^{-3} when α is larger than 1.65. In summary, the BER performance becomes good as α increases in all cases, but the system will become unsecure when α is too large. Therefore, both BER performance and security should be considered. In our experiment, the measure range α is from 0.85 to 1.95; when α is between 1.65 and 1.95, the BER of the decrypted signal after 100-km transmission is less than 3.8×10^{-3}, and the BER of the encrypted signal in the BtB case is larger than 3.8×10^{-3}. Therefore, when α is larger than 1.65 and less than 1.95, 100-km chaos-based secure optical transmission can be realized with the BER less than 3.8×10^{-3}.

In conclusion, by using the duobinary modulation format, a 10-GHz chaotic carrier is used to encrypt the 30 Gb/s signal, which alleviates the requirement for wideband chaos synchronization in high-speed chaotic optical communications; in the meantime, this proposal simplified the strict dispersion compensation for a wideband chaotic carrier in long-distance transmission. Therefore, a 30 Gb/s signal over 100-km SMF secure transmission with BER below 3.8×10^{-3} has been realized, and the BER transmission performance in BtB and 100-km transmission cases has been studied. In addition, TDC and DCF are used for dispersion compensation, while EDFA is used for the compensation of IL, which means the system is compatible with traditional commercial optical communication systems. We hope this proposal can pave the way for high-speed long-distance secure communications.

Funding. National Natural Science Foundation of China (NSFC) (61575122).

REFERENCES

1. L. M. Pecora and T. L. Carroll, Phys. Rev. Lett. **64**, 821 (1990).
2. G. D. VanWiggeren and R. Roy, Science **279**, 1198 (1998).
3. I. Fischer, Y. Liu, and P. Davis, Phys. Rev. A **62**, 011801 (2000).
4. S. Sivaprakasam and K. A. Shore, IEEE J. Quantum Electron. **36**, 35 (2000).
5. V. Annovazzi-Lodi, S. Donati, and A. Scirè, IEEE J. Quantum Electron. **33**, 1449 (1997).
6. J. P. Goedgebuer, L. Larger, and H. Porte, Phys. Rev. Lett. **80**, 2249 (1998).
7. J. P. Goedgebuer, P. Levy, L. Larger, C. C. Chen, and W. T. Rhodes, IEEE J. Quantum Electron. **38**, 1178 (2002).
8. N. Gastaud, S. Poinsot, L. Larger, J. M. Merolla, M. Hanna, J. P. Goedgebuer, and F. Malassenet, Electron. Lett. **40**, 898 (2004).
9. A. Argyris, D. Syvridis, L. Larger, V. Annovazzi-Lodi, P. Colet, I. Fischer, J. García-Ojalvo, C. R. Mirasso, L. Pesquera, and K. A. Shore, Nature **438**, 343 (2005).
10. R. Lavrov, M. Peil, M. Jacquot, L. Larger, V. Udaltsov, and J. Dudley, Phys. Rev. E **80**, 026207 (2009).
11. R. Lavrov, M. Jacquot, and L. Larger, IEEE J. Quantum Electron. **46**, 1430 (2010).
12. J. Z. Ai, L. L. Wang, and J. Wang, Opt. Lett. **42**, 3662 (2017).
13. J. Oden, R. Lavrov, Y. K. Chembo, and L. Larger, Chaos **27**, 114311 (2017).
14. N. Jiang, C. Wang, C. P. Xue, G. L. Li, S. Q. Lin, and K. Qiu, Opt. Express **25**, 14359 (2017).
15. A. B. Wang, Y. B. Yang, B. J. Wang, B. B. Zhang, L. Li, and Y. C. Yang, Opt. Express **21**, 8701 (2013).
16. A. B. Wang, Y. C. Wang, Y. B. Yang, M. J. Zhang, H. Xu, and B. J. Wang, Appl. Phys. Lett. **102**, 031112 (2013).
17. C. Cheng, Y. Chen, and F. Lin, Opt. Express **23**, 2308 (2015).
18. P. Pablo and A. Valle, IEEE J. Quantum Electron. **51**, 2400207 (2015).
19. Y. Hong, P. S. Spencer, and K. A. Shore, IEEE J. Quantum Electron. **50**, 236 (2014).
20. R. M. Nguimdo, R. Lavrov, P. Colet, M. Jacquot, Y. K. Chembo, and L. Larger, J. Lightwave Technol. **28**, 2688 (2010).